

Research Article

Comprehensive Design Criteria and Analysis of Laser Communication System for Underwater Vehicles

Ibrahim Emirhan Delibas and Alper Nabi Akpolat

Abstract— Underwater vehicles are utilized in various fields, such as exploration, submarine research, and industrial applications. However, underwater communication is often a formidable challenge because conventional communication technologies are ineffective for underwater vehicles. Therefore, laser communication systems for underwater vehicles are receiving more and more attention. This paper presents a novel approach by investigating comprehensive design criteria and analysis of laser communication systems for underwater vehicles. Firstly, the basic principles and working mechanisms of underwater laser communication systems are explained. Then, the main factors affecting system performance and design criteria are discussed in detail. These criteria include communication distance, data rate, power consumption, optical properties of the underwater environment, and system stability. Different laser modulation techniques and communication protocols are also evaluated. The paper also focuses on simulation, channel diversity, and test methods that can be used to assess the performance of laser communication systems in different underwater environments.

Index Terms— Laser communication, underwater vehicles, data flow, bit error rate (BER), quality (Q) factor.

I. INTRODUCTION

IN TODAY'S technology, wired communication has been replaced by wireless communication. Laser communication is preferred in remote distances and places where wiring is not feasible due to environmental conditions. Additionally, the reasons for the preference for laser communication are its faster speed than wired communication and the absence of wiring costs. Underwater communication systems are widely used in military, research, and exploration applications. Various data transmission methods transmit data underwater, such as acoustic, radio frequency, and optical communication. Communication methods using acoustic and radio frequencies

are more vulnerable due to high error rates, inability to achieve high data transmission speeds, and susceptibility to cyber-attacks [1]. Radiofrequency and acoustic communication systems underwater communicate with high error rates, low data rates, and limited bandwidth. In such scenarios, optical communication emerges as a viable alternative. Optical communication is preferable for long-distance communication underwater due to features such as light's ability to transmit data at high bandwidth, low latency, high reliability, and low error rates. With this motivation, we design an underwater communication system. This system aims to achieve low error rates and high-quality (Q) factor results in various underwater environments at different distances. This study constructs a fundamental model for defense applications, underwater research, and marine sciences.

Research [2] has presented that amplitude modulation (AM) and frequency modulation (FM) methods transmit signals with distortion. In contrast, phase modulation (PM) and frequency-shift keying (FSK) are more susceptible to phase variations. They used a modulated laser diode (MLD) to generate a laser beam with disruption, and the incoming signals were analyzed using NI myDAQ. In [3], the selection of the transmitter for Free Space Optics (FSO) communication is explored during weather conditions. It compares wavelengths from 1550 nm to 10000 nm.

Similarly, [4] delved into modulation methods employed in communication and evaluated their highest achievable data rates over a distance of 45,000 km. The findings suggest that coherent optical (CO) frequency-shift keying (PSK) performs with the 850 nm wavelength, outperforming the 1064 nm and 1550 nm wavelengths. Furthermore, a simulative analysis of 10 Gbps bandwidth using optical communication channels has been conducted, comparing three optical channels: Optical Wireless Communication (OWC), FSO, Line-of-Sight Free Space Optics (LOS-FSO), using quadrature amplitude modulation (QAM) and PSK modulation formats [5]. A different study has been proposed for underwater visible light communication (UVLC) systems operation, having established that the performance of UVLC is influenced by factors such as receiver transmitter, water type, etc. [6]. Also, this article achieves a high optical density using a UVLC circuit over long distances with the help of Monte Carlo simulations [7]. A gradual attenuation channel is modeled to address the complex nature of vertical underwater links, where water temperature and salinity gradients in various water layers are used to

Ibrahim Emirhan DELİBAŞ, is with the Department of Electrical-Electronics Engineering, Marmara University, Istanbul, Türkiye, (e-mail: idelibas@marun.edu.tr).

 <https://orcid.org/0009-0007-9561-7538>

Alper Nabi AKPOLAT, is with the Department of Electrical-Electronics Engineering, Marmara University, Istanbul, Türkiye, (e-mail: alper.nabi@marmara.edu.tr).

 <https://orcid.org/0000-0002-6972-2509>

Manuscript received Jul 13, 2024; accepted Feb 12, 2025.

DOI: [10.17694/bajece.1515423](https://doi.org/10.17694/bajece.1515423)

consider different attenuation coefficients, with real-time data transmission underwater [8].

The primary goal of this study is to provide a basic methodology that meets the comprehensive design criteria and analysis of laser communication systems for underwater vehicles. The study elaborates on the basic principles, operating mechanisms, and main factors affecting the performance and design criteria of UVLC. One crucial contribution is providing an essential resource for researchers, engineers, and students interested in designing and implementing laser communication systems. It also discusses an example of laser communication on system design and analysis aspects of current technology, future research areas, and development opportunities. This provides essential information for developing more efficient and reliable systems for underwater communications.

The rest of this study is organized as follows: Section II describes a general overview of laser communication systems for FSO and underwater communication. Section III gives the design steps of the proposed system. Section IV explains the findings and discussions that were obtained. Section V provides the conclusion and future remarks.

II. GENERAL OVERVIEW OF LASER COMMUNICATION SYSTEMS

With capabilities such as high-speed data transfer, increased bandwidth, reduced bit error rates, and overall cabling costs, all laser communication systems are at the forefront of communication systems. They are the most preferred option when the distance is too long or cabling could be more convenient. A typical system used in laser communications is FSO.

A. Free Space Optics (FSO)

FSO is a communication method that utilizes light transmission in free space for data transmission. It involves transmitting data through a void, air, or space-like environment. FSO is preferred in environments unsuitable for using fiber optic cables or systems requiring high costs [9]. The attenuation coefficient varies depending on the conditions of the transmission medium. Table I shows the attenuation coefficients in the FSO communication environment.

TABLE I
WEATHER ATTENUATION FOR FSO [10].

Weather Conditions	α (dB/km)
Heavy fog	125
Moderate fog	42.2
Light fog	20
Heavy rain	9.2
Moderate rain	5.8
Haze	4.2
Clear air	0.43

The Beer-Lambert law gives the following formula for the power of light transmitted through free space.

$$I = I_0 \times e^{-kd} \tag{1}$$

where, k is the attenuation coefficient of the medium, d is the length of the medium, I is light power, and I_0 is incoming laser power.

B. Underwater Optic Communication

Underwater Optical Communication (UOC) is a form of communication in which light propagates through the underwater environment for data transmission. This communication type is used in underwater research and exploration applications, where environmental conditions are not conducive to cabling, and high data rates and wide bandwidth are needed. Similar to FSO, light in UOC is subject to the attenuation coefficient of the medium extinction, scattering, and absorption coefficients for different types of water are provided in Table II.

TABLE II
EXTINCTION, SCATTERING AND ABSORPTION COEFFICIENT FOR DIFFERENT TYPES OF WATER [11-13].

Type of Water	Extinction coefficient (c) (m^{-1})	Scattering coefficient (b) (m^{-1})	Absorption coefficient (α) (m^{-1})
Harbor	1.1	0.913	0.187
Pure Sea	0.043	0.0025	0.0405
Clear Ocean	0.151	0.037	0.114
Coastal Ocean	0.398	0.219	0.179

$$c(\lambda) = \alpha(\lambda) + b(\lambda) \tag{2}$$

Three different modulation techniques, Mach-Zehnder (MZ) modulation, electro-absorption (EA) modulation, and AM, have been investigated to validate the comprehension design for laser communication systems for underwater vehicles.

III. DESIGN STEPS, CIRCUIT DESCRIPTION, AND FORMULATION OF STUDIED SYSTEM

A. System Modeling and Simulation

The general system design is a 1 Watt-480 nm pure sea environment, as given in Fig. 1. It was created using the OptiSystem software environment. The system sends data in bit form with a test pattern to convert to an electrical square wave using the NRZ pulse generator component. The NRZ Pulse Generator produces square wave signals according to the following formulations.

$$\text{Exponential } E(t) \begin{cases} 1 - e^{-(t/c_r)}, 0 \leq t < t_1 \\ 1, t_1 \leq t < t_2 \\ e^{-(t/c_f)}, t_2 \leq t < T \end{cases} \tag{3}$$

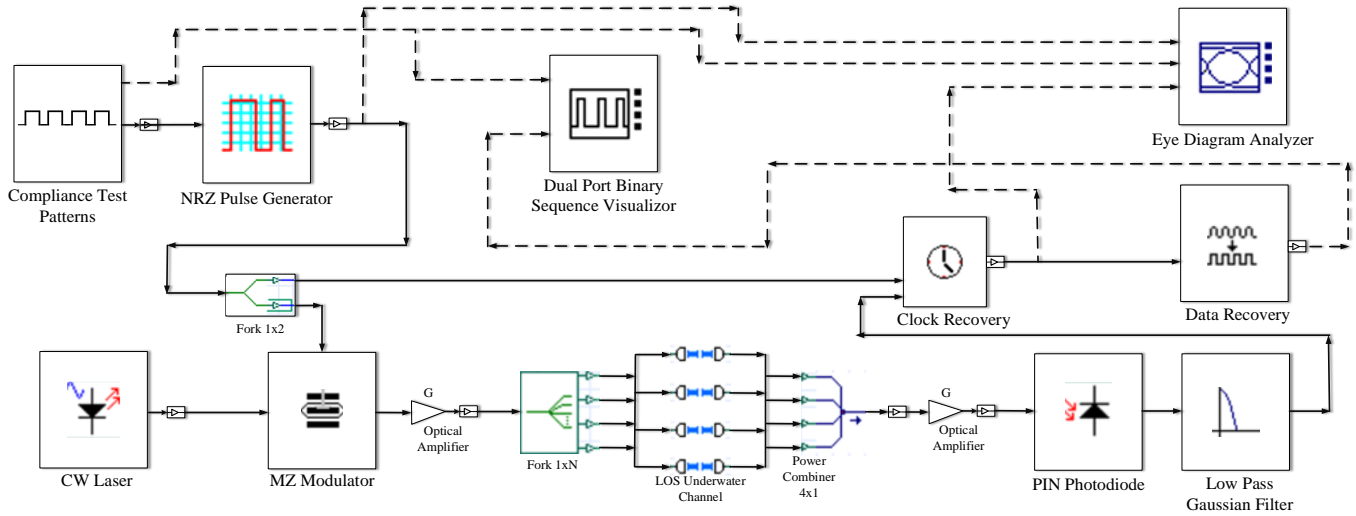


Fig. 1. System design of underwater laser communication in pure sea.

$$\text{Gaussian } E(t) \begin{cases} 1 - e^{-(t/c_r)^2}, & 0 \leq t < t_1 \\ 1, & t_1 \leq t < t_2 \\ e^{-(t/c_f)^2}, & t_2 \leq t < T \end{cases} \quad (4)$$

$$\text{Linear } E(t) \begin{cases} t/c_r, & 0 \leq t < t_1 \\ 1, & t_1 \leq t < t_2 \\ t/c_f, & t_2 \leq t < T \end{cases} \quad (5)$$

$$\text{Sine. } E(t) \begin{cases} \sin(\pi t/c_r), & 0 \leq t < t_1 \\ 1, & t_1 \leq t < t_2 \\ \sin(\pi t/c_f), & t_2 \leq t < T \end{cases} \quad (6)$$

$$\alpha = 1 - \frac{4}{\pi} \cdot \arctan\left(\frac{1}{\sqrt{ER}}\right) \quad (9)$$

$$\Delta\phi(t) = SC \cdot \Delta\theta(t) \cdot (1 + SF) / (1 - SF) \quad (10)$$

where, SF is the symmetry factor, SC is equal to minus one (-1) if the negative signal chirp is true or one of the negative signal chirp is false. ER is the signal extinction ratio, and $Modulation(t)$ is the modulating input signal. The electrical input modulating signal is normalized internally between 1 and 0. The general scheme of the EA modulator is seen in Fig. 3.

where, the rising time coefficient is c_r , the fall time coefficient is c_f , and the bit period is T . The parameters rising time and fall time values are used to numerically set the time numerically points t_1 and t_2 , as well as c_r and c_f , to produce pulses. The generated square wave signal is modulated with an MZ modulator using a CW optical laser signal. Data is converted to an optical signal using three different types of modulators. Modulators regarding MZ, EA, and AMAX Fig 2 shows the general scheme of the MZ Modulator.

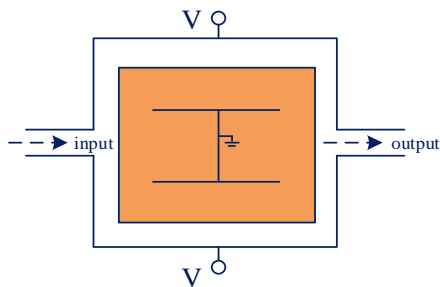


Fig. 2. General overview of MZ modulation.

$$E_{out}(t) = E_{in}(t) \cdot \cos(\Delta\theta(t)) \cdot \exp(j \cdot \Delta\phi(t)) \quad (7)$$

$$\Delta\theta(t) = \frac{\pi}{2} \cdot (0.5 - \alpha \cdot (Modulation(t) - 0.5)) \quad (8)$$

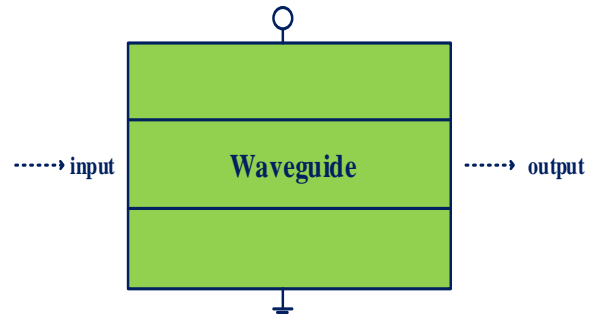


Fig. 3. General overview of EA modulation.

$$E_{out}(t) = E_{in}(t) \cdot \sqrt{Mod(t)} \cdot \exp\left(j \frac{\alpha}{2} \cdot \ln(Mod(t))\right) \quad (11)$$

where, $E_{in}(t)$ is the input signal, $E_{out}(t)$ is the output optical signal, and α is the chirp factor.

$$Mod(t) = (1 - MI) + MI \cdot modulation(t) \quad (12)$$

where, $modulation(t)$ is the input signal and MI is the modulation index.

- AM Modulator,

$$E_{out}(t) = E_{in}(t) \cdot \sqrt{Mod(t)} \quad (13)$$

where, $E_{in}(t)$ is the input signal, $E_{out}(t)$ is the output optical signal,

$$Mod(t) = (1 - MI) + MI \cdot modulation(t) \quad (14)$$

where, $modulation(t)$ is the input signal and MI is the modulation index.

The modulated optical signal is amplified using an Optical Amplifier (OA). The reason for using OA is that our transmitted laser signal will be subjected to various noise and attenuation in the underwater channel, so it is necessary to introduce a high-power signal into this channel. The goal is to limit the power of our laser source to a certain level and then amplify it using OA. The modulated and amplified optical signal is split into multiple channels using a Power Splitter and transmitted through four lines of sight (LOS) underwater channels.

$$G = \frac{(P_{OUT} - P_{ASE})}{P_{in}} \quad (15)$$

where, G is gain, P_{out} is the total output power, P_{in} is the total input power, and P_{ASE} includes (or does not include) the generated Amplified Spontaneous Emission (ASE).

$$P_{R_los} = P_r \eta_r \eta_R \exp\left[-c(\lambda) \frac{d}{\cos(\theta)}\right] \frac{A_{Rec} \cos(\theta)}{2\pi d^2 [1 - \cos(\theta_0)]} \quad (16)$$

where, the laser beam divergence angle is θ_0 , the receiver aperture area is A_{Rec} , the perpendicular distance between the transmitter and the receiver plane is d , the optical efficiency of the transmitter is ηT , and the angle between the transmitter-receiver trajectory and the receiver plane is θ .

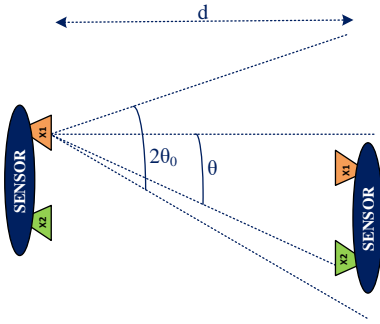


Fig. 4. LOS underwater channel model [14].

Fig. 4 depicts the optical signal transmitted through the LOS Underwater channel, which undergoes attenuation. After being amplified again with an OA, it is converted to an electrical signal using the Pin Photodiode component, as depicted in Fig. 5.

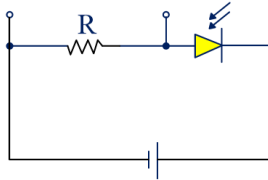


Fig. 5. Pin photodiode circuit.

$$i(t) = rP(t) + i_d \quad (17)$$

$$\sigma_{total}^2 = \sigma_{th}^2 + \sigma_{shot-S}^2 + \sigma_{shot-ASE}^2 + \sigma_{S-ASE}^2 + \sigma_{ASE-ASE}^2 \quad (18)$$

$$\sigma_{shot-S}^2 = 2B_e \cdot (rP_s + i_d) \quad (Shot - Signal Noise) \quad (19)$$

$$\sigma_{shot-ASE}^2 = 2B_e \cdot qrP_{ASE} \quad (Shot - ASE Noise) \quad (20)$$

$$\sigma_{S-ASE}^2 = 4B_e \cdot r^2 \cdot PSD_{ASE} \cdot P_s \quad (Signal - ASE Noise) \quad (21)$$

$$\sigma_{ASE-ASE}^2 = r^2 \cdot PSD_{ASE}^2 \quad (ASE - ASE Beat Noise) \quad (22)$$

where, B_e is the PIN's equivalent noise bandwidth, r is its responsivity, q is its electron charge value, i_d is its dark current, P_s is its signal power, P_{ASE} is its optical noise power, and PSD_{ASE} is its power spectrum density of the optical noise field (spontaneous emission). The received electrical signal is filtered with a Gaussian low-pass frequency function.

$$H(f) = \alpha e^{-\ln(\sqrt{2}) \left(\frac{f}{f_c}\right)^{2N}} \quad (23)$$

where, N is the parameter for Order, α is the parameter for Insertion loss, f is the frequency, $H(f)$ is the filter transfer function, and f_c is the filter cutoff frequency. The filtered electrical signal is equalized in time with the input signal using the Clock Recovery component. Then, the electrical signal is converted to binary data using the Data Recovery component, allowing for comparison between the transmitted and received binary data. The Input and Output signals are compared using the Eye Diagram Analyzer component to obtain parameters such as Q Factor, Min BER, and Max Eye Height and to generate an eye diagram.

IV. RESULTS AND DISCUSSIONS

Before reaching the optimum system design, scenarios were conducted to find the optimal configuration, and each scenario's results are as follows.

In the first scenario, measurements were taken in the system using MZ modulation with a 1-Watt 532 nm wavelength laser; the PIN photodiode's parameters are responsivity 0.5 and dark current 2 nA, and the low-pass Gaussian filter's cutoff frequency = 0.75 * symbol rate in a Pure Sea environment without using an OA. The other scenarios use the same parameters as the first scenario. Data transmission was performed and compared. The system design of the first scenario can be seen in Fig. 6. The transmitted signal did not adequately reach the receiver in the constructed circuit. The eye diagram output is shown in Fig. 7.

In the second scenario, in addition to the setup in the first scenario, two OAs were added, one at the input and one at the output of the transmission channel. The OA parameters are gain 40 dB and noise Fig. 4 dB. The system design of the second scenario is shown in Fig. 8. As a result of the scenario, the transmitted signal reached the receiver properly, and the Q factor value was measured as 282.337. The eye diagram result is given in Fig. 9.

In the third scenario, when the parameters used in the second scenario system design were simulated in a clear ocean environment, the data was not adequately transmitted to the receiver. The eye diagram result is given in Fig. 10.

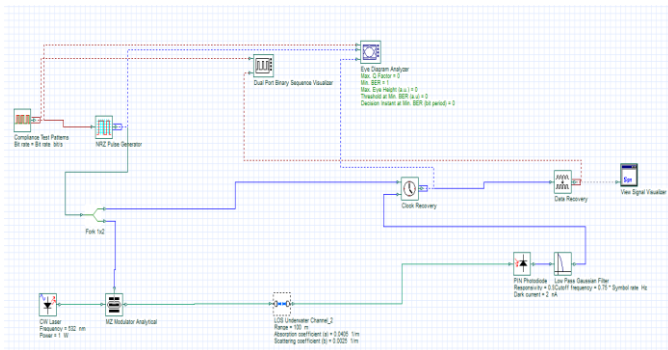


Fig. 6. System design for the first scenario.

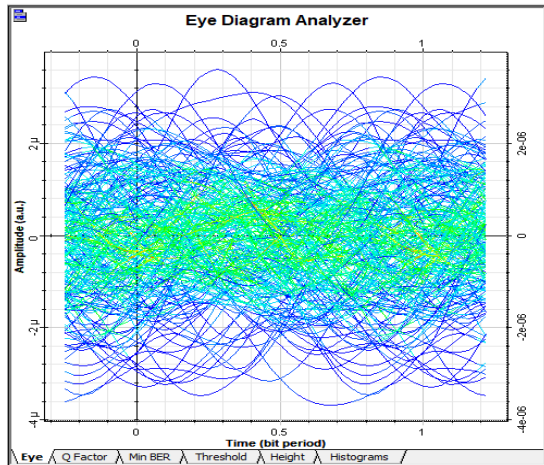


Fig. 7. Eye diagram for the first scenario.

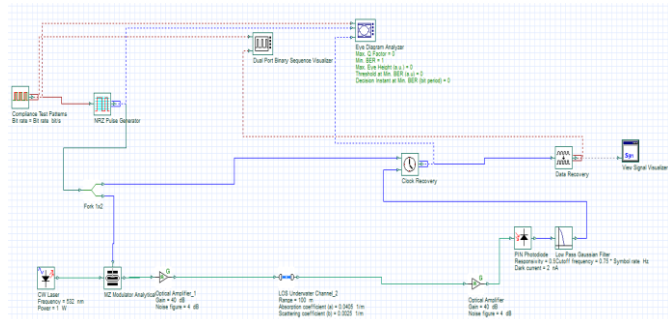


Fig. 8. System design for the second scenario.

In the fourth scenario, the signal was correctly transmitted when the number of transmission channels was increased to 4. The system design of the fourth scenario is shown in Fig. 11. Considering the result for the fourth scenario, Fig. 12 expresses the eye diagram result. The scenarios determined that the optimal circuit design was created with four channels and OA. In the optimal circuit design simulation, two different channels were simulated in the underwater transmission channel: Pure Sea and Clear Ocean. Simulations were conducted with three different modulations at a fixed distance of 100 meters and other wavelengths. The Min BER and Max (M) Q factor values of the transmitted data in these channels with two different attenuation coefficients were measured, and eye diagram graphs were generated.

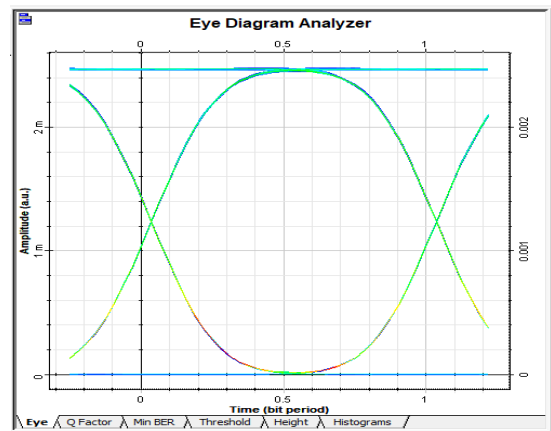


Fig. 9. Eye diagram for the second scenario.

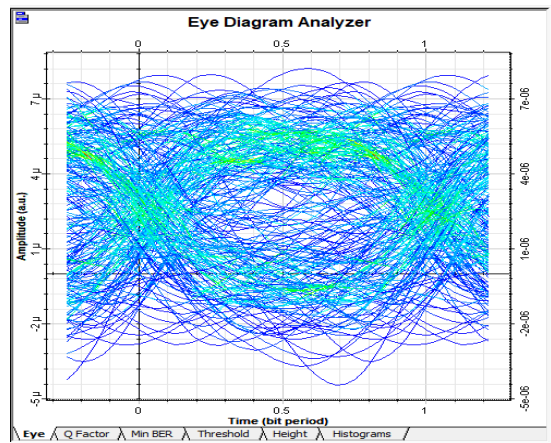


Fig. 10. Eye diagram for the third scenario.

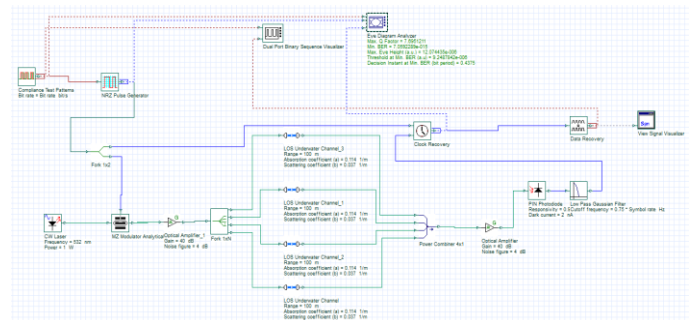


Fig. 11. System design for the fourth scenario.

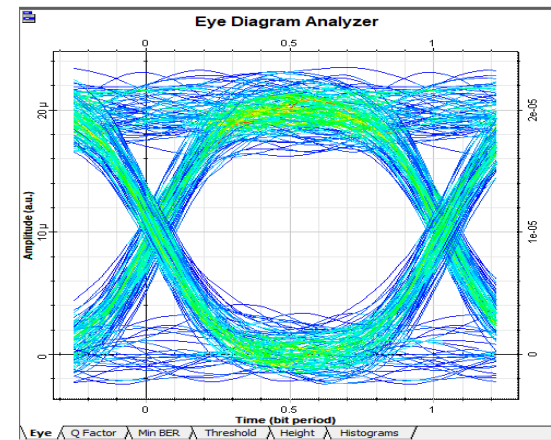


Fig. 12. Eye diagram for the fourth scenario.

TABLE III

PURE SEA, 100 METERS, 1 WATT LASER POWER.

		WAVELENGTH (nm)						
		405	532	635	980	1064	1550	
MODULATION TYPE	MZ	Max Q Factor:	354.082	355.331	353.365	353.583	352.925	123.632
		Eye Height:	0.97191	0.971923	0.971884	0.971895	0.971871	0.956203
		Min BER :	0	0	0	0	0	0
	EA	Max Q Factor:	344.753	344.87	345.883	345.232	346.688	99.1558
		Eye Height:	0.9248	0.924788	0.924822	0.924807	0.924838	0.904289
		Min BER :	0	0	0	0	0	0
	AM	Max Q Factor:	343.996	345.439	344.573	346.414	345.723	115.545
		Eye Height:	0.973449	0.973485	0.973471	0.973515	0.973482	0.956898
		Min BER :	0	0	0	0	0	0

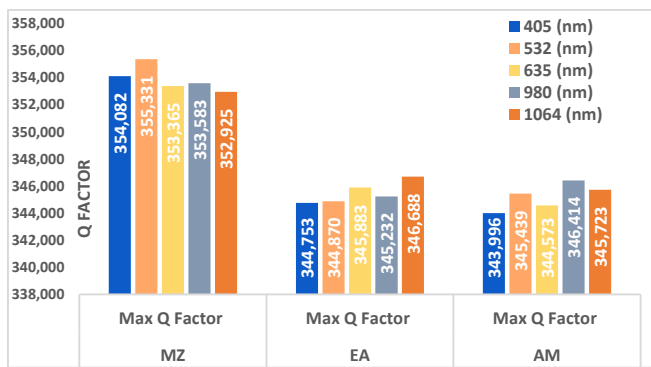


Fig. 13. Q factor table for Pure Sea environment.

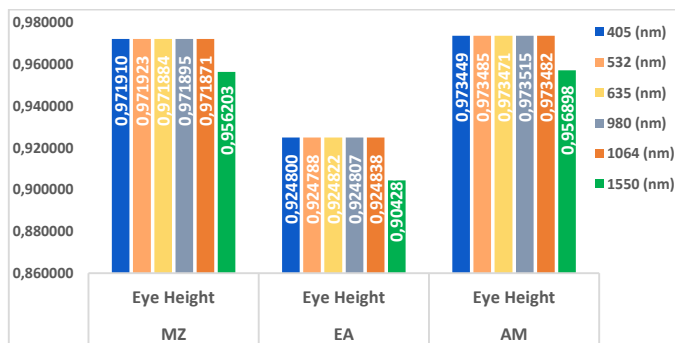


Fig. 14. Eye height table for Pure Sea environment.

As shown in Fig. 13, using MZ modulation and a 532 nm wavelength laser resulted in a higher Q factor in the pure sea environment compared to other scenarios.

Fig. 14 displays that using AM modulation and a 1064 nm wavelength laser resulted in a higher eye height in the pure sea environment than in other scenarios.

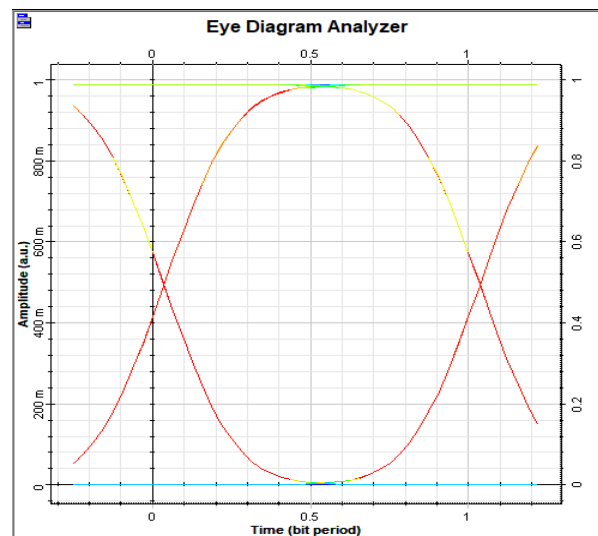


Fig. 15. Eye diagram for Pure Sea environment with MZ modulation (532 nm wavelength).

The scenario conducted in the Pure Sea environment achieved the best result using MZ modulation and a wavelength of 532 nm. The eye diagram of the best scenario can be observed in Fig. 15. As can be seen in Table III, 18 different parameters for the pure sea environment are obtained. Fig. 16 shows that using AM modulation and a 1064 nm wavelength laser resulted in a higher Q factor in the clear ocean environment compared to other scenarios. As seen in Fig. 17, using AM modulation and a 1064 nm wavelength laser resulted in a lower Min BER in the clear ocean environment compared to the other scenarios. Fig. 18 shows that using EA modulation and a 980 nm wavelength laser resulted in a higher eye height in the clear ocean environment compared to different scenarios.

TABLE IV
CLEAR OCEAN, 100 METERS, 1 WATT LASER POWER.

		WAVELENGTH (nm)					
		405	532	635	980	1064	1550
MODULATION TYPE	MZ	Max Q Factor:	Max Q Factor:	Max Q Factor:	Max Q Factor:	Max Q Factor:	Max Q Factor: 0
		7.71839	7.26355	7.55246	8.22645	8.01527	
		Eye Height :	Eye Height :	Eye Height :	Eye Height :	Eye Height:	Eye Height : 0
	1.1279e-05	1.16268e-05	1.2028e-05	1.29086e-05	1.24512e-05		
	Min BER:	Min BER :	Min BER :	Min BER :	Min BER :	Min BER : 1	
	5.86909e-15	1.88525e-13	2.12939e-14	9.52291e-17	5.46291e-16		
	EA	Max Q Factor:	Max Q Factor:	Max Q Factor:	Max Q Factor:	Max Q Factor:	Max Q Factor: 0
		7.23672	7.50535	7.48618	7.11237	8.26744	
		Eye Height:	Eye Height:	Eye Height:	Eye Height:	Eye Height:	Eye Height : 0
1.10836e-05	1.12577e-05	1.14245e-05	1.08784e-05	1.2367e-05			
Min BER :	Min BER :	Min BER :	Min BER :	Min BER :	Min BER : 1		
2.2752e-13	3.05014e-14	3.51692e-14	5.599e-14	6.83795e-17			
AM	Max Q Factor:	Max Q Factor:	Max Q Factor:	Max Q Factor:	Max Q Factor:	Max Q Factor: 0	
	7.31086	7.97961	8.05461	8.23974	8.61914		
	Eye Height:	Eye Height:	Eye Height:	Eye Height:	Eye Height:	Eye Height : 0	
1.27444e-05	1.06522e-05	1.24187e-05	1.26896e-05	1.29787e-05			
Min BER:	Min BER :	Min BER :	Min BER :	Min BER :	Min BER : 1		
4.66896e-17	7.20103e-16	3.95456e-16	8.52336e-17	3.29406e-18			

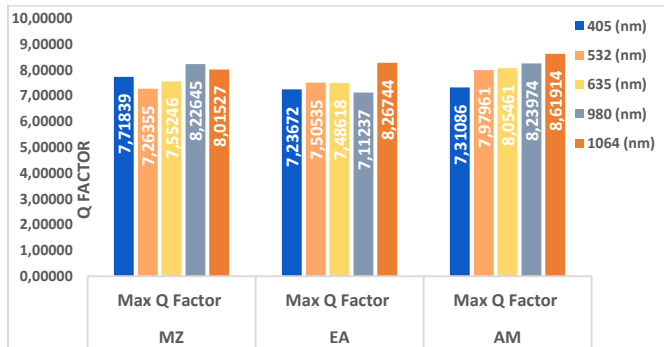


Fig. 16. Q factor table for Clear Ocean environment.

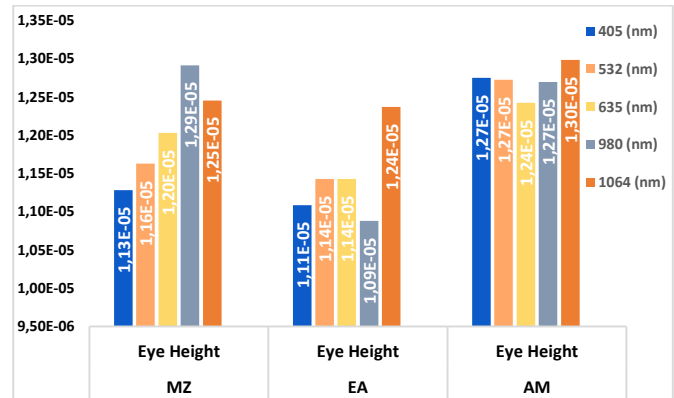


Fig. 18. Eye height table for Clear Ocean environment.

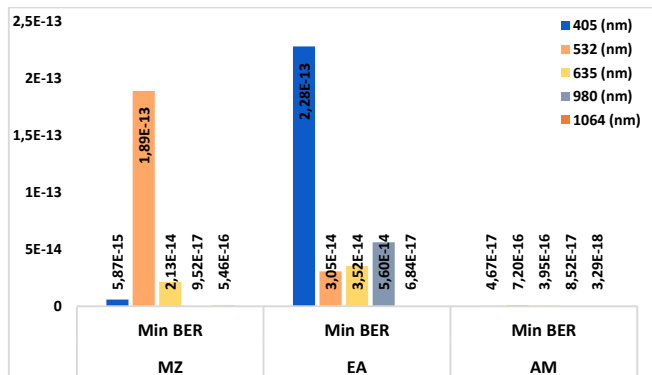


Fig. 17. Min BER table for Clear Ocean environment.

The scenario conducted in the Clear Ocean environment achieved the best result using AM modulation and a wavelength of 1064 nm. The eye diagram of the best scenario is shown in Fig. 19.

Similarly, Table IV presents the max Q factor, eye height, and min BER parameters for a clear ocean environment. Upon reviewing the findings presented in the article, it becomes evident that using optical amplifiers while transmitting data over long distances via laser, both in pure sea and clear ocean environments, ensures a more stable delivery of data to the receiving end. It has been observed that transmitting data over multiple channels rather than a single channel enhances data quality. Additionally, it has been determined that high-wavelength lasers transfer data more effectively in environments with high coefficient values.

V. CONCLUSION AND FUTURE REMARKS

Considering all the experimental results conducted in both pure sea and clear ocean environments, the results of 1550 nm laser were worse than the results of lasers with other wavelengths.

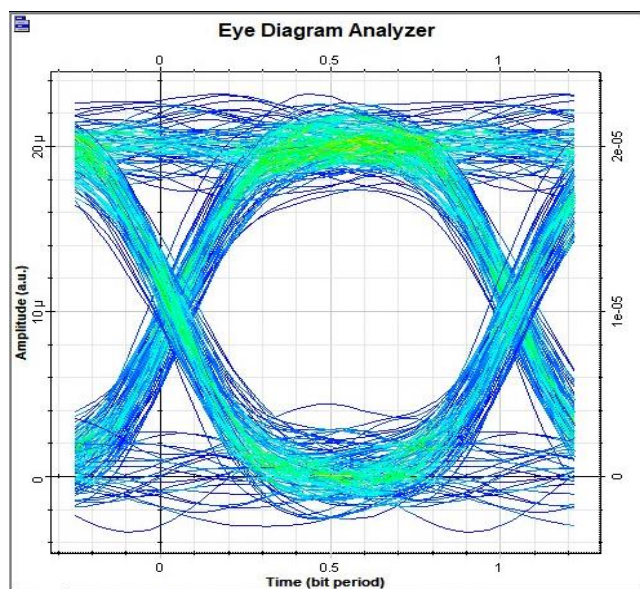


Fig. 19. Eye diagram for Clear Ocean environment with AM modulation (1064 nm wavelength).

Therefore, it has been understood that utilizing lasers with a wavelength of 1550 nm for underwater optical communication is not preferable to lasers with other wavelengths. Briefly, this paper presents an example of laser communication system design and analysis based on current technology and discusses future research areas and development opportunities. It will be a valuable resource for researchers and engineers interested in designing and implementing laser communication systems to meet the communication needs of underwater vehicles.

VI. ACKNOWLEDGEMENT

The authors would like to extend their sincere thanks to HAVELSAN for their supportive approaches.

REFERENCES

- [1] P. K. Pandey, "MIMO based high-speed underwater optical wireless communication using WDM," *2022 IEEE International Students' Conference on Electrical, Electronics and Computer Science (SCEECS)*, BHOPAL, India, 2022, pp. 1-5.
- [2] MAX R. Alam and S. Faruque, "Comparison of different modulation techniques for free space laser communication," *2015 IEEE International Conference on Electro/Information Technology (EIT)*, Dekalb, IL, USA, 2015, pp. 637-640, doi: 10.1109/EIT.2015.7293409.
- [3] P. Singal, S. Rai, R. Punia, and D. Kashyap, "Comparison of Different Transmitters Using 1550nm and 10000nm in FSO Communication Systems," *International Journal of Computer Science & Information Technology (IJCSIT)*, vol. 7, no. 3, June 2015.
- [4] J. Kaur, B. Kaur, and K. Singh, "Design and Performance Investigation of Intersatellite Optical Wireless Communication System Employing Modulation Techniques," *Wireless Personal Communication*, vol. 94, pp. 793-807, 2017.
- [5] G. Karpagarajesh, R. Santhana Krishnan, Y. Harold Robinson, S. Vimal, S. Kadry, and Y. Nam, "Investigation of digital video broadcasting application employing the modulation formats like QAM and PSK using OWC, FSO, and LOS-FSO channels," *Alexandria Eng. J.* vol. 61, no. 1, pp. 647-657, 2022.
- [6] MAX Elamassie, F. Miramirkhani, and MAX Uysal, "Performance Characterization of Underwater Visible Light Communication," *IEEE Transactions on Communications*, vol. 67, no. 1, pp. 543-552, Jan. 2019.
- [7] C. Wang, H -Y. Yu, and Y. -J. Zhu, "A Long Distance Underwater Visible Light Communication System With Single Photon Avalanche Diode," *IEEE Photonics Journal*, vol. 8, no. 5, pp. 1-11, Oct. 2016.

- [8] MAX Elamassie and MAX Uysal, "Vertical Underwater Visible Light Communication Links: Channel Modeling and Performance Analysis," *IEEE Transactions on Wireless Communications*, vol. 19, no. 10, pp. 6948-6959, Oct. 2020.
- [9] S. A. Al-Gailani et al., "A Survey of Free Space Optics (FSO) Communication Systems, Links, and Networks," *IEEE Access*, vol. 9, pp. 7353-7373, 2021.
- [10] A. Mansour, R. Mesleh, and MAX Abaza, "New Challenges in Wireless & Free Space Optical Communications," *Optics and Lasers in Engineering*, vol. 89 pp. 95-108, 2017.
- [11] R. Boluda-Ruiz, P. Rico-Pinazo, B. Castillo-Vázquez, A. Garcia-Zambrana, and K. Qaraq, "Impulse Response Modeling of Underwater Optical Scattering Channels for Wireless Communication," *IEEE Photonics Journal*, vol. 12, no. 4, pp. 1-14, Aug. 2020.
- [12] C. D. Mobley *Light and Water: Radiative Transfer in Natural Waters*. New York, NY, USA: Academic, 1994.
- [13] V. I. Haltrin, "Chlorophyll-based model of seawater optical properties," *Appl. Opt.*, vol. 38, No. 33, pp. 6826-6832, 1999.
- [14] S. Arnon, "Optical wireless communication," *Encyclopedia of Optical Engineering*, vol. 2, pp. 1866-1886, 2003.

BIOGRAPHIES

Ibrahim Emirhan DELIBAS received the B.Sc. and MSc. degrees in the Department of Electrical-Electronics Engineering from Marmara University, Istanbul, Turkiye, in 2019 and 2024, respectively. He currently works as a software engineer in the defense industry.



Alper Nabi Akpolat received the B.Sc. and the MSc. degrees from Firat University, Elazig, Turkiye, in 2012 and 2015, respectively. He also received his Ph.D. degree from Marmara University in 2021. He works as an Assistant Professor in the Department of Electrical-Electronics Engineering at the same University, Istanbul, Turkiye. Since



March 2019, he has been a Guest Ph.D. student for one year with the Department of Energy Technology, Aalborg University, Denmark. His current research interests include renewable energy systems, PV systems, DC microgrids, control of distributed generation systems, green hydrogen production, neural networks, and applied artificial intelligence in power electronics and power systems.